Artificial Boundary Method for Anisotropic Problems in an Unbounded Domain with a Concave Angle

Yajun Chen, and Qikui Du

Abstract—**In this paper, the artificial boundary method for anisotropic problems in an infinite domain with a concave angle is investigated. The exact and approximate boundary conditions on an artificial boundary are given. Finite element approximations are applied to the problem in a bounded computational domain and error estimates are obtained. Finally, some numerical examples show the effectiveness of this method.**

Index Terms—**artificial boundary method, anisotropic problem, error estimate.**

I. Introduction

In scientific and engineering computing, many problems can be modeled by boundary value problems of partial differential equations in unbounded domains. Artificial boundary method [1]-[2], which is also called coupling method with natural boundary reduction [3]-[5] or DtN method [6]-[7] is a common method to solve such problems numerically. The method may be summarized as follows: (i) Introduce an artificial boundary, which divides the original unbounded domain into two non-overlapping subdomains: a bounded computational domain and an infinite residual domain. (ii) By analyzing the problem in the infinite residual domain, obtain a relation on the artificial boundary involving the unknown function and its derivatives. (iii) Using the relation as a boundary condition, to obtain a well-posed problem in the bounded computational domain. (iv) Solve the problem in the bounded computational domain be the standard finite element methods or some other numerical methods.

In the past three decades, artificial boundaries of various shapes have been derived for problems in unbounded domains. Circular [8]-[9] and elliptical [10]-[12] artificial boundaries for two dimensional exterior problems; spheroidal [13] and ellipsoidal [14] artificial boundaries for three dimensional exterior problems; circular arc artificial boundaries for linear [15]-[16] and quasilinear [17] problems in concave angle domains. Other related works may also be found from [18]-[21].

Recently, the authors used a new elliptical arc artificial boundary to solve Poisson problems in concave angle domains [22]. In this paper, we follow the idea of [22] for solving some anisotropic problems in an unbounded domain with a concave angle. Let Ω be an exterior concave angle domain with angle ω, and $0 < \omega \leqslant 2\pi$. The boundary of domain Ω is decomposed into three disjoint parts: Γ, Γ_0 and Γ_ω(see Fig. 1), i.e. $\partial\Omega = \overline{\Gamma \cup \Gamma_0 \cup \Gamma_\omega}$, $\Gamma_0 \cap \Gamma_\omega = \emptyset$, $\Gamma \cap \Gamma_0 = \emptyset$, $\Gamma \cap \Gamma_\omega = \emptyset$. The boundary Γ is a simple smooth curve part, Γ_0 and Γ_ω are two half lines.

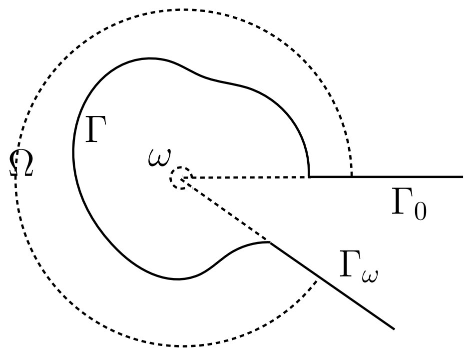

Fig. 1. The Illustration of Domain Ω

We consider the following anisotropic problems in two cases:

$$\begin{cases} -\nabla \cdot (\mathcal{A}\nabla u) = f, & \text{in } \Omega, \\ \mathcal{A}\nabla u \cdot n = 0, & \text{on } \Gamma_0 \cup \Gamma_\omega, \\ u = g, & \text{on } \Gamma, \\ u \text{ is bounded at infinity}, \end{cases} \tag{1}$$

and

$$\begin{cases} -\nabla \cdot (\mathcal{A}\nabla u) = f, & \text{in } \Omega, \\ u = 0, & \text{on } \Gamma_0 \cup \Gamma_\omega, \\ \mathcal{A}\nabla u \cdot n = h, & \text{on } \Gamma, \\ u \text{ is vanish at infinity}, \end{cases} \tag{2}$$

where $\mathcal{A} = \begin{pmatrix} k^2 & 0 \\ 0 & 1 \end{pmatrix}$, k is a constant and $0 < k < 1$, u is the unknown function, $f \in L^2(\Omega)$ and $g, h \in L^2(\Gamma)$ are given functions, supp(f) is compact.

The rest of the paper is organized as follows. In section 2, we obtain the exact artificial boundary condition. In section 3, we give the equivalent variational problem and it's well-posedness. In section 4, we discuss the finite element approximation and an new error estimate that depends on the finite element mesh, the order of artificial boundary condition and the location of the artificial boundary. Finally, in section 5, we give some numerical examples to show the effectiveness of the method.

Manuscript received April 23, 2016; revised August 26, 2016. This work was supported by the National Natural Science Foundation of China (Grant No. 11371198).

Yajun Chen is with the School of Mathematical Sciences, Nanjing Normal University, Nanjing 210023 and the Department of Mathematics, Shanghai Maritime University, Shanghai 200136, China. (E-mail: chenyajun@shmtu.edu.cn).

Qikui Du is with the School of Mathematical Sciences, Nanjing Normal University, Nanjing 210023, China.

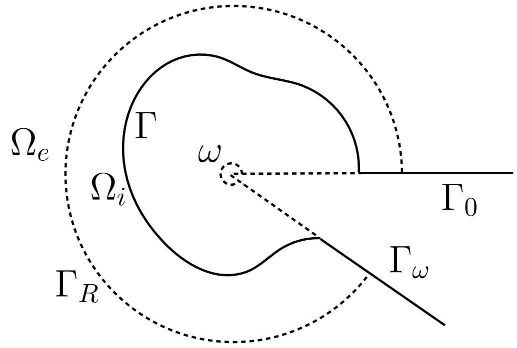

Fig. 2. The Illustration of Domain Ω_i and Ω_e

II. THE EXACT ARTIFICIAL BOUNDARY CONDITION

We introduce an circular arc artificial boundary $\Gamma_R = \{(x,y)|x^2+y^2=R^2,\ (x,y)\in\Omega\}$ to enclose supp(f), which divides Ω into a bounded domain Ω_i and an unbounded domain Ω_e(see Fig. 2).

In the first case, problem (1) confines in Ω_i is

$$\begin{cases} -\nabla\cdot(\mathcal{A}\nabla u)=f, \quad \text{in } \Omega_i, \\ \mathcal{A}\nabla u\cdot n=0, \quad \text{on } \Gamma_{0i}\cup\Gamma_{\omega i}, \\ u=g, \quad \text{on } \Gamma, \end{cases} \tag{3}$$

where $\Gamma_{0i}=\Gamma_0\cap\Omega_i$, $\Gamma_{\omega i}=\Gamma_\omega\cap\Omega_i$.

Problem (1) confines in Ω_e is

$$\begin{cases} -\nabla\cdot(\mathcal{A}\nabla u)=0, \quad \text{in } \Omega_e, \\ \mathcal{A}\nabla u\cdot n=0, \quad \text{on } \Gamma_{0e}\cup\Gamma_{\omega e}, \\ u \text{ is bounded at infinity}, \end{cases} \tag{4}$$

where $\Gamma_{0e}=\Gamma_0\cap\Omega_e$, $\Gamma_{\omega e}=\Gamma_\omega\cap\Omega_e$.

By the variable transform $x=k\xi$, $y=\eta$, the anisotropic equation becomes a Poisson equation in $\widetilde{\Omega}$ and the circular arc boundary Γ_R becomes an elliptical arc boundary $\widetilde{\Gamma}_R=\{(\xi,\eta)|k^2\xi^2+\eta^2=R^2,\ (\xi,\eta)\in\widetilde{\Omega}\}$. Let f_0 denote the half distance between the two foci of an ellipse, we introduce an elliptic system of co-ordinates (μ,φ) such that the artificial boundary $\widetilde{\Gamma}_R$ coincides with the elliptical arc $\{(\mu,\varphi)|\mu=\mu_R, 0<\varphi<\omega\}$, where $f_0=\frac{\sqrt{1-k^2}}{k}R$ and $\mu_R=\ln\frac{1+k}{\sqrt{1-k^2}}$. Thus, the Cartesian co-ordinates (ξ,η) are related to the elliptic co-ordinates (μ,φ) , that is $\xi=f_0\cosh\mu\cos\varphi$, $\eta=f_0\sinh\mu\sin\varphi$.

Problem (3) becomes the following problem

$$\begin{cases} -\Delta u=f, \quad \text{in } \widetilde{\Omega}_i, \\ \dfrac{\partial u}{\partial n}=0, \quad \text{on } \widetilde{\Gamma}_{0i}\cup\widetilde{\Gamma}_{\omega i}, \\ u=g, \quad \text{on } \widetilde{\Gamma}. \end{cases} \tag{5}$$

Problem (4) becomes the following problem

$$\begin{cases} -\Delta u=0, \quad \text{in } \widetilde{\Omega}_e, \\ \dfrac{\partial u}{\partial n}=0, \quad \text{on } \widetilde{\Gamma}_{0e}\cup\widetilde{\Gamma}_{\omega e}, \\ u \text{ is bounded at infinity}, \end{cases} \tag{6}$$

where $\widetilde{\Omega}_e=\{(\mu,\varphi)|\mu>\mu_R, 0<\varphi<\omega\}$, $\widetilde{\Gamma}_{0e}=\{(\mu,\varphi)|\mu>\mu_R,\varphi=0\}$, $\widetilde{\Gamma}_{\omega e}=\{(\mu,\varphi)|\mu>\mu_R,\varphi=\omega\}$.

By separation of variables, we know that the solution of problem (6) has the form

$$u(\mu,\varphi)=\frac{a_0}{2}+\sum_{n=1}^{+\infty}a_n e^{(\mu_R-\mu)\frac{n\pi}{\omega}}\cos\frac{n\pi\varphi}{\omega}, \tag{7}$$

where

$$a_n=\frac{2}{\omega}\int_0^\omega u(\mu_R,\phi)\cos\frac{n\pi\phi}{\omega}d\phi, \quad n=0,1,2,\cdots\cdots. \tag{8}$$

We differentiate (7) with respect to μ and set $\mu=\mu_R$ to obtain

$$\frac{\partial u}{\partial\mu}|_{\widetilde{\Gamma}_R}=-\frac{2\pi}{\omega^2}\sum_{n=1}^{+\infty}n\int_0^\omega u(\mu_R,\phi)\cos\frac{n\pi\varphi}{\omega}\cos\frac{n\pi\phi}{\omega}d\phi. \tag{9}$$

Since

$$\frac{\partial u}{\partial n}|_{\widetilde{\Gamma}_R}=-\frac{1}{\sqrt{J}}\frac{\partial u}{\partial\mu}|_{\widetilde{\Gamma}_R},$$

where $J=\frac{R^2}{k^2}(\sin^2\varphi+k^2\cos^2\varphi)$, we obtain the exact artificial boundary condition on $\widetilde{\Gamma}_R$

$$\begin{aligned}\frac{\partial u}{\partial n}|_{\widetilde{\Gamma}_R}&=\frac{2\pi}{\omega^2\sqrt{J}}\sum_{n=1}^{+\infty}n\int_0^\omega u(\mu_R,\phi)\cos\frac{n\pi\varphi}{\omega}\cos\frac{n\pi\phi}{\omega}d\phi\\&\triangleq\mathcal{K}_1u(\mu_R,\varphi).\end{aligned} \tag{10}$$

In practice, we need to truncate the above infinite series by finite terms, let

$$\mathcal{K}_1^N=\frac{2\pi}{\omega^2\sqrt{J}}\sum_{n=1}^{N}n\int_0^\omega u(\mu_R,\phi)\cos\frac{n\pi\varphi}{\omega}\cos\frac{n\pi\phi}{\omega}d\phi, \tag{11}$$

then we obtain the approximate artificial boundary condition on $\widetilde{\Gamma}_R$

$$\frac{\partial u}{\partial n}|_{\widetilde{\Gamma}_R}=\mathcal{K}_1^N. \tag{12}$$

For the second case, the exact artificial boundary condition on $\widetilde{\Gamma}_R$ is

$$\begin{aligned}\frac{\partial u}{\partial n}|_{\widetilde{\Gamma}_R}&=\frac{2\pi}{\omega^2\sqrt{J}}\sum_{n=1}^{+\infty}n\int_0^\omega u(\mu_R,\phi)\sin\frac{n\pi\varphi}{\omega}\sin\frac{n\pi\phi}{\omega}d\phi\\&\triangleq\mathcal{K}_2u(\mu_R,\varphi),\end{aligned} \tag{13}$$

and the approximate artificial boundary condition on $\widetilde{\Gamma}_R$ is

$$\begin{aligned}\frac{\partial u}{\partial n}|_{\widetilde{\Gamma}_R}&=\frac{2\pi}{\omega^2\sqrt{J}}\sum_{n=1}^{N}n\int_0^\omega u(\mu_R,\phi)\sin\frac{n\pi\varphi}{\omega}\sin\frac{n\pi\phi}{\omega}d\phi\\&\triangleq\mathcal{K}_2^N.\end{aligned} \tag{14}$$

In the following sections, we just consider the equivalent variational problem and finite element approximation of problem (1), we can obtain corresponding result of problem (2) in the same way.

III. The equivalent variational problem

By the exact artificial boundary condition (10), the original problem (1) confines in $\widetilde{\Omega}_i$ is

$$\begin{cases} -\Delta u = f, \quad \text{in } \widetilde{\Omega}_i, \\ \dfrac{\partial u}{\partial n} = 0, \quad \text{on } \widetilde{\Gamma}_{0i} \cup \widetilde{\Gamma}_{\omega i}, \\ u = g, \quad \text{on } \widetilde{\Gamma}, \\ \dfrac{\partial u}{\partial n} = \mathcal{K}_1 u(\mu_R, \varphi), \quad \text{on } \widetilde{\Gamma}_R. \end{cases} \tag{15}$$

By the approximate artificial boundary condition (12), the approximation problem can be described as follows

$$\begin{cases} -\Delta u^N = f, \quad \text{in } \widetilde{\Omega}_i, \\ \dfrac{\partial u^N}{\partial n} = 0, \quad \text{on } \widetilde{\Gamma}_{0i} \cup \widetilde{\Gamma}_{\omega i}, \\ u^N = g, \quad \text{on } \widetilde{\Gamma}, \\ \dfrac{\partial u^N}{\partial n} = \mathcal{K}_1^N, \quad \text{on } \widetilde{\Gamma}_R. \end{cases} \tag{16}$$

Let $V = H^1(\widetilde{\Omega}_i)$, $V_g = \{v \in H^1(\widetilde{\Omega}_i), v|_{\widetilde{\Gamma}} = g\}$, then the problem (15) is equivalent to the following variational problem

$$\begin{cases} \text{Find } u \in V_g, \text{ such that} \\ a(u,v) + b(u,v) = f(v), \quad \forall v \in V_0, \end{cases} \tag{17}$$

problem (16) is equivalent to the following variational problem

$$\begin{cases} \text{Find } u^N \in V_g, \text{ such that} \\ a(u^N,v) + b_N(u^N,v) = f(v), \quad \forall v \in V_0, \end{cases} \tag{18}$$

where

$$a(u,v) = \int_{\Omega_i} \mathcal{A}\nabla u \cdot \nabla v dxdy = k\int_{\widetilde{\Omega}_i} \nabla u \cdot \nabla v d\xi d\eta, \tag{19}$$

$$\begin{aligned} b(u,v) =& k\sum_{n=1}^{+\infty} \frac{2}{n\pi} \int_0^\omega \int_0^\omega \frac{\partial u(\mu_R,\phi)}{\partial \phi} \frac{\partial v(\mu_R,\varphi)}{\partial \varphi} \\ & \cdot \sin\frac{n\pi\varphi}{\omega} \sin\frac{n\pi\phi}{\omega} d\phi d\varphi, \end{aligned} \tag{20}$$

$$\begin{aligned} b_N(u,v) =& k\sum_{n=1}^{N} \frac{2}{n\pi} \int_0^\omega \int_0^\omega \frac{\partial u(\mu_R,\phi)}{\partial \phi} \frac{\partial v(\mu_R,\varphi)}{\partial \varphi} \\ & \cdot \sin\frac{n\pi\varphi}{\omega} \sin\frac{n\pi\phi}{\omega} d\phi d\varphi, \end{aligned} \tag{21}$$

$$f(v) = \int_{\Omega_i} fv dxdy = k\int_{\widetilde{\Omega}_i} fv d\xi d\eta. \tag{22}$$

For any real number s, we have the equivalent definition of Sobolev spaces $H^s(\widetilde{\Gamma}_R)$ as follows [19]:

$$\forall v \in H^s(\widetilde{\Gamma}_R) \Leftrightarrow v(\mu_R,\varphi) = \frac{c_0}{2} + \sum_{n=1}^{+\infty} c_n \cos\frac{n\pi\varphi}{\omega},$$

$$\text{and } \frac{c_0^2}{2} + \sum_{n=1}^{+\infty} (1+n^2)^s c_n^2 < \infty.$$

The norm of $H^s(\widetilde{\Gamma}_R)$ can be defined as follows

$$\|v(\mu_R,\varphi)\|_{s,\widetilde{\Gamma}_R} = [\frac{c_0^2}{2} + \sum_{n=1}^{+\infty}(1+n^2)^s c_n^2]^{\frac{1}{2}}.$$

Then we have the following results.

Lemma 1. $b(u,v)$ and $b_N(u,v)$ are both a symmetric, semi-definite and continuous bilinear form on $V \times V$.

Proof. Let

$$u(\mu_R,\phi) = \frac{a_0}{2} + \sum_{n=1}^{+\infty} a_n \cos\frac{n\pi\phi}{\omega},$$

$$v(\mu_R,\varphi) = \frac{c_0}{2} + \sum_{n=1}^{+\infty} c_n \cos\frac{n\pi\varphi}{\omega},$$

taking the derivative with respect to ϕ and φ we have

$$\frac{\partial u(\mu_R,\phi)}{\partial\phi} = \sum_{n=1}^{+\infty} \frac{n\pi}{\omega} a_n \sin\frac{n\pi\phi}{\omega},$$

$$\frac{\partial v(\mu_R,\varphi)}{\partial\varphi} = \sum_{n=1}^{+\infty} \frac{n\pi}{\omega} c_n \sin\frac{n\pi\varphi}{\omega},$$

then we have

$$\begin{aligned} |b(u,v)| &= |\frac{k\pi}{2}\sum_{n=1}^{+\infty} n a_n c_n| \\ &\le \frac{k\pi}{2}\|u\|_{\frac{1}{2},\widetilde{\Gamma}_{\mu_R}} \|v\|_{\frac{1}{2},\widetilde{\Gamma}_{\mu_R}} \\ &\le C\|u\|_{1,\widetilde{\Omega}_i}\|v\|_{1,\widetilde{\Omega}_i}. \end{aligned}$$

In the same way, we obtain

$$|b_N(u,v)| = |\frac{k\pi}{2}\sum_{n=1}^{N} n a_n c_n| \le C\|u\|_{1,\widetilde{\Omega}_i}\|v\|_{1,\widetilde{\Omega}_i},$$

$$|b(u,u)| = \frac{k\pi}{2}\sum_{n=1}^{+\infty} n a_n^2 \ge 0,$$

$$|b_N(u,u)| = \frac{k\pi}{2}\sum_{n=1}^{N} n a_n^2 \ge 0.$$

By using this lemma we have the following theorem.

Theorem 1. The variational problem (17) and (18) have a unique solution on V, respectively.

Proof. It is easy to see that $a(u,v)$ is a symmetric, bounded and coercive bilinear form on $V \times V$. Note that $f(v)$ is a continuous linear function on V and lemma 1, we completed the prove of this theorem by Lax-Milgram theorem.

IV. Finite Element Approximation

Assume that $\mathcal{J}_h$ is a regular and quasi-uniform triangulation of $\widetilde{\Omega}_i$ such that

$$\widetilde{\Omega}_i = \bigcup_{K\in\mathcal{J}_h} K,$$

where K is a (curved) triangle and h is the maximal diameter of the triangles. For the sake of simplicity, we assume $g = 0$. Let

$$V_h = \{v \in V_0, v|_K \text{ is a linear polynomial}, \ \forall K \in \mathcal{J}_h\}.$$

The approximation problem of (18) can be described as follows

$$\begin{cases} \text{Find } u_h^N \in V_h, \text{ such that} \\ a(u_h^N,v) + b_N(u_h^N,v) = f(v), \quad \forall v \in V_h. \end{cases} \tag{23}$$

Similar with theorem 1, we can see that the variational problem (23) has a unique solution $u_h^N \in V_h$.

Let $\widetilde{\Gamma}_{\mu_0} = \{(\mu_0, \varphi)|\mu_0 < \mu_R, 0 < \varphi < \omega\}$ be the smallest elliptical arc to enclose supp(f), we have

Lemma 2. Suppose u is the solution of the problem (1), $u|_{\widetilde{\Gamma}_{\mu_0}} \in H^{p-\frac{1}{2}}(\widetilde{\Gamma}_{\mu_0})$, p is a constant and $p \geq 1$, then for any $v \in V$ we have

$$|b_N(u,v) - b(u,v)| \leq C\frac{e^{(\mu_0-\mu_R)\frac{(N+1)\pi}{\omega}}}{(N+1)^{p-1}}\|u\|_{p-\frac{1}{2},\widetilde{\Gamma}_{\mu_0}}\|v\|_{1,\widetilde{\Omega}_i}, \tag{24}$$

where C is a constant independent of h, N and μ_R.

Proof. By the formula (7) we have

$$u(\mu_0, \phi) = \frac{a_0}{2} + \sum_{n=1}^{+\infty} a_n e^{(\mu_0-\mu_R)\frac{n\pi}{\omega}} \cos\frac{n\pi\phi}{\omega}.$$

For any $v \in V$, let

$$v(\mu_R, \varphi) = \frac{e_0}{2} + \sum_{n=1}^{+\infty} e_n \cos\frac{n\pi\varphi}{\omega}.$$

Then we have

$$\begin{aligned}
&|b_N(u,v) - b(u,v)| \\
&= |\sum_{n=N+1}^{+\infty} \frac{2k}{n\pi}\int_0^\omega\int_0^\omega \frac{\partial u}{\partial\phi}\frac{\partial v}{\partial\varphi}\sin\frac{n\pi\varphi}{\omega}\sin\frac{n\pi\phi}{\omega}d\phi d\varphi| \\
&= |\frac{k\pi}{2}\sum_{n=N+1}^{+\infty} nc_n e^{(\mu_0-\mu_R)\frac{n\pi}{\omega}} e_n| \\
&\leq \frac{k\pi e^{(\mu_0-\mu_R)\frac{(N+1)\pi}{\omega}}}{2(N+1)^{p-1}}|\sum_{n=N+1}^{+\infty} n^p c_n e_n| \\
&\leq C\frac{e^{(\mu_0-\mu_R)\frac{(N+1)\pi}{\omega}}}{(N+1)^{p-1}}\|u\|_{p-\frac{1}{2},\widetilde{\Gamma}_{\mu_0}}\|v\|_{1,\widetilde{\Omega}_i}.
\end{aligned}$$

Theorem 2. Suppose $u \in H^2(\widetilde{\Omega}_i)$ is a solution of the problem (1), $u|_{\widetilde{\Gamma}_{\mu_0}} \in H^{p-\frac{1}{2}}(\widetilde{\Gamma}_{\mu_0})$, p is a constant and $p \geq 1$, $u_h^N \in V_h$ is the solution of the problem (23), the following error estimate holds

$$\|u - u_h^N\|_{1,\widetilde{\Omega}_i} \leq C(h\|u\|_{2,\widetilde{\Omega}_i} + \frac{e^{(\mu_0-\mu_R)\frac{(N+1)\pi}{\omega}}}{(N+1)^{p-1}}\|u\|_{p-\frac{1}{2},\widetilde{\Gamma}_{\mu_0}}), \tag{25}$$

where C is a constant independent of h, N and μ_R.

Proof. From variational problem (17) and (18) we have

$$\begin{aligned}
&a(u-u_h^N, v) + b_N(u-u_h^N, v) \\
&= b_N(u,v) - b(u,v), \quad \forall v \in V_h.
\end{aligned}$$

For $\forall v \in V_h$, by lemma 2 we have

$$\begin{aligned}
&\|u_h^N - v\|^2_{1,\widetilde{\Omega}_i} \\
&\leq C(a(u_h^N - v, u_h^N - v) + b_N(u_h^N - v, u_h^N - v)) \\
&= C(a(u - v, u_h^N - v) + b_N(u - v, u_h^N - v) \\
&\quad + b(u, u_h^N - v) - b_N(u, u_h^N - v)) \\
&\leq C(\|u - v\|_{1,\widetilde{\Omega}_i}\|u_h^N - v\|_{1,\widetilde{\Omega}_i} \\
&\quad + |b(u, u_h^N - v) - b_N(u, u_h^N - v)|) \\
&\leq C(\|u - v\|_{1,\widetilde{\Omega}_i}\|u_h^N - v\|_{1,\widetilde{\Omega}_i} \\
&\quad + \frac{e^{(\mu_0-\mu_R)\frac{(N+1)\pi}{\omega}}}{(N+1)^{p-1}}\|u\|_{p-\frac{1}{2},\widetilde{\Gamma}_{\mu_0}}\|u_h^N - v\|_{1,\widetilde{\Omega}_i}).
\end{aligned}$$

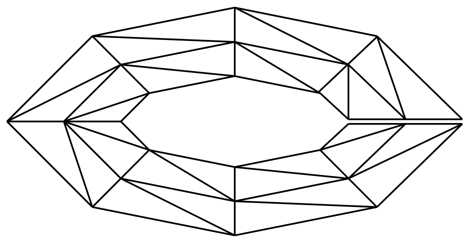

Fig. 3. Mesh h of Subdomain $\widetilde{\Omega}_i$ for Example 1

Therefore,

$$\begin{aligned}
&\|u_h^N - v\|_{1,\widetilde{\Omega}_i} \leq C(\|u - v\|_{1,\widetilde{\Omega}_i} \\
&+ \frac{e^{(\mu_0-\mu_R)\frac{(N+1)\pi}{\omega}}}{(N+1)^{p-1}}\|u\|_{p-\frac{1}{2},\widetilde{\Gamma}_{\mu_0}}), \quad \forall v \in V_h.
\end{aligned}$$

Notice that

$$\inf_{v\in V_h}\|u - v\|_{1,\widetilde{\Omega}_i} \leq Ch\|u\|_{2,\widetilde{\Omega}_i},$$

and by the triangle inequality

$$\|u - u_h^N\|_{1,\widetilde{\Omega}_i} \leq \|u - v\|_{1,\widetilde{\Omega}_i} + \|u_h^N - v\|_{1,\widetilde{\Omega}_i},$$

we obtain

$$\begin{aligned}
&\|u - u_h^N\|_{1,\widetilde{\Omega}_i} \\
&\leq C(h\|u\|_{2,\widetilde{\Omega}_i} + \frac{e^{(\mu_0-\mu_R)\frac{(N+1)\pi}{\omega}}}{(N+1)^{p-1}}\|u\|_{p-\frac{1}{2},\widetilde{\Gamma}_{\mu_0}}).
\end{aligned}$$

V. Numerical examples

We computed two numerical examples to test the effectiveness of the method we developed. The finite element method with linear elements is used in the computation.

Example 1. We consider problem (1), where $\Omega = \{(r,\theta)|r > 1, 0 < \theta < 2\pi\}$, $\Gamma = \{(1,\theta)|0 < \theta < 2\pi\}$, $\Gamma_0 = \{(r,0)|r > 1\}$ and $\Gamma_\omega = \{(r,2\pi)|r > 1\}$. By using coordinate transformation $x = k\xi$, $y = \eta$, we turn the original problem into the problem as the following

$$\begin{cases}
-\Delta u = f, \quad \text{in } \widetilde{\Omega}, \\
\dfrac{\partial u}{\partial n} = 0, \quad \text{on } \widetilde{\Gamma}_0 \cup \widetilde{\Gamma}_\omega, \\
u = g, \quad \text{on } \widetilde{\Gamma},
\end{cases} \tag{26}$$

where $\widetilde{\Omega} = \{(\mu,\varphi)|\mu > \mu_0, 0 < \varphi < 2\pi\}$, $\widetilde{\Gamma} = \{(\mu_0,\varphi)|0 < \varphi < 2\pi\}$, $\widetilde{\Gamma}_0 = \{(\mu,0)|\mu > \mu_0\}$, $\widetilde{\Gamma}_\omega = \{(\mu,2\pi)|\mu > \mu_0\}$, $f_0 = \frac{\sqrt{1-k^2}}{k}$ and $\mu_0 = \ln\frac{1+k}{\sqrt{1-k^2}}$. Let $u(x,y) = \frac{k^2x}{x^2+k^2y^2}$ be the exact solution of original problem and $g = u|_{\widetilde{\Gamma}}$. Take the confocal elliptical arc artificial boundary $\widetilde{\Gamma}_R = \{(\mu_R,\varphi)|\mu_R > \mu_0, 0 < \varphi < 2\pi\}$. Fig. 3 shows the Mesh h of subdomain $\widetilde{\Omega}_i$ with $k = 0.7$ and $\mu_R = 2\mu_0$, Table 1 shows $L^\infty(\widetilde{\Omega}_i)$ errors with different Mesh($N = 20$, $\mu_R = 2\mu_0$), Fig. 4 shows $L^\infty(\widetilde{\Omega}_i)$ errors with different N($k = 0.7$, $\mu_R = 2\mu_0$), Fig. 5 shows $L^\infty(\widetilde{\Omega}_i)$ errors with different μ_R($k = 0.7$, $N = 20$).

Example 2. We consider problem (1), where $\Omega = \{(r,\theta)|r > 1, 0 < \theta < \frac{3\pi}{2}\}$, $\Gamma = \{(1,\theta)|0 < \theta < \frac{3\pi}{2}\}$, $\Gamma_0 = \{(r,0)|r > 1\}$ and $\Gamma_\omega = \{(r,\frac{3\pi}{2})|r > 1\}$. By using coordinate transformation $x = k\xi$, $y = \eta$, we turn the original problem into the problem (26), where $\widetilde{\Omega} = \{(\mu,\varphi)|\mu > \mu_0, 0 < \varphi < \frac{3\pi}{2}\}$, $\widetilde{\Gamma} = \{(\mu_0,\varphi)|0 < \varphi <$

TABLE I
$L^\infty(\widetilde{\Omega}_i)$ ERRORS WITH DIFFERENT MESH FOR EXAMPLE 1

Mesh	$k=0.9$	$k=0.8$	$k=0.7$	$k=0.6$	$k=0.5$
h	0.06753	0.06250	0.05850	0.05482	0.04406
$h/2$	0.01564	0.01509	0.01377	0.01386	0.01838
$h/4$	0.00383	0.00374	0.00338	0.00355	0.00427
$h/8$	0.00095	0.00093	0.00085	0.00088	0.00104

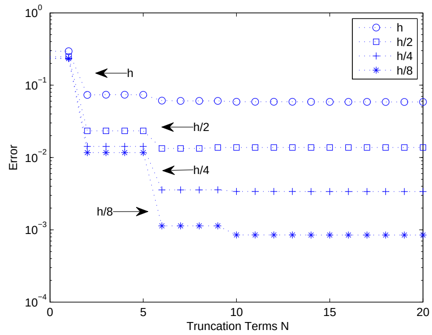

Fig. 4. $L^\infty(\widetilde{\Omega}_i)$ Errors with Different N for Example 1

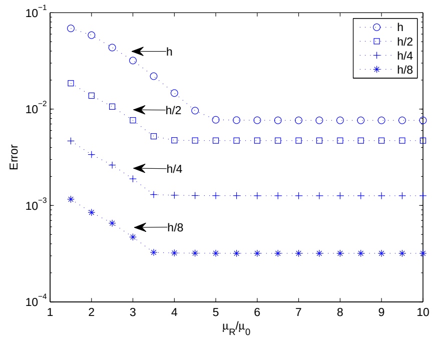

Fig. 5. $L^\infty(\widetilde{\Omega}_i)$ Errors with Different μ_R for Example 1

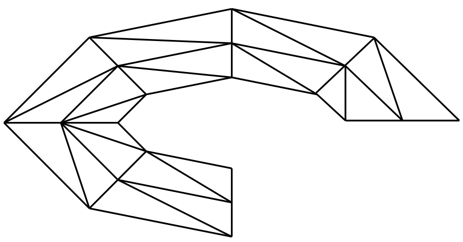

Fig. 6. Mesh h of Subdomain $\widetilde{\Omega}_i$ for Example 2

$\frac{3\pi}{2}\}$, $\widetilde{\Gamma}_0 = \{(\mu, 0)|\mu > \mu_0\}$, $\widetilde{\Gamma}_\omega = \{(\mu, \frac{3\pi}{2})|\mu > \mu_0\}$, $f_0 = \frac{\sqrt{1-k^2}}{k}$ and $\mu_0 = \ln \frac{1+k}{\sqrt{1-k^2}}$. Let $u(x,y) = \frac{k^3(x^2-y^2)}{(x^2+k^2y^2)^2}$ be the exact solution of original problem and $g = u|_{\widetilde{\Gamma}}$. Take the confocal elliptical arc artificial boundary $\widetilde{\Gamma}_R = \{(\mu_R, \varphi)|\mu_R > \mu_0, 0 < \varphi < \frac{3\pi}{2}\}$. Fig. 6 shows the Mesh h of subdomain $\widetilde{\Omega}_i$ with $k = 0.5$ and $\mu_R = 2\mu_0$, Table 2 shows $L^\infty(\widetilde{\Omega}_i)$ errors with different Mesh($N = 20$, $\mu_R = 2\mu_0$), Fig. 7 shows $L^\infty(\widetilde{\Omega}_i)$ errors with different $N(k = 0.5$, $\mu_R = 2\mu_0)$, Fig. 8 shows $L^\infty(\widetilde{\Omega}_i)$ errors with different $\mu_R(k = 0.5,\ N = 20)$.

The numerical results show that the numerical errors can be affected by the finite element mesh, the order of artificial boundary condition and the location of artificial boundary.

TABLE II
$L^\infty(\widetilde{\Omega}_i)$ ERRORS WITH DIFFERENT MESH FOR EXAMPLE 2

Mesh	$k=0.5$	$k=0.4$	$k=0.3$	$k=0.2$	$k=0.1$
h	0.26521	0.35362	0.44868	0.54528	0.64360
$h/2$	0.05326	0.09611	0.17849	0.32838	0.53118
$h/4$	0.01219	0.02046	0.04087	0.10945	0.37038
$h/8$	0.00299	0.00490	0.00914	0.02527	0.17152

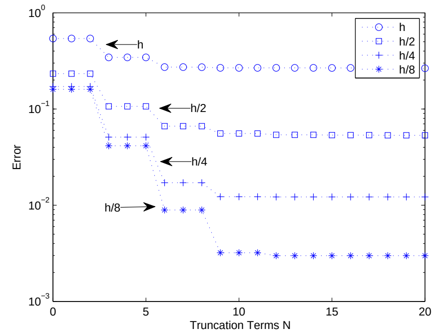

Fig. 7. $L^\infty(\widetilde{\Omega}_i)$ Errors with Different N for Example 2

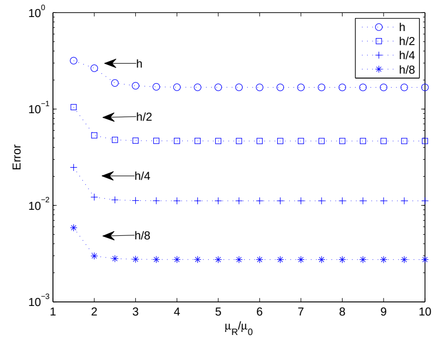

Fig. 8. $L^\infty(\widetilde{\Omega}_i)$ Errors with Different μ_R for Example 2

Numerical results are in agreement with the error estimates and show the efficiency of our method.

ACKNOWLEDGMENT

The authors would like to thank the reviewers for their valuable comments which improve the paper.

REFERENCES

[1] H. Han, and X. Wu, "Approximation of Infinite Boundary Condition and Its Application to Finite Element Methods," Journal of Computational Mathematics, vol. 3, no. 2, pp179-192, 1985

[2] H. Han, and X. Wu, The Artificial Boundary Method – Numerical Solutions of Partial Differential Equations on Unbounded Domains, Tsinghua University Press, Beijing, 2009

[3] K. Feng, "Finite Element Method and Natural Boundary Reduction," in Proceedings of the International Congress Mathematicians 1983, ICM 1983, August 16-24, 1983, Warszawa, pp1439-1453

[4] K. Feng, and D. Yu, "Canonical Integral Equations of Elliptic Boundary Value Problems and Their Numerical Solutions," in Proceedings of China-France Symposium on the Finite Element Methods 1983, CFSFEM 1983, April 19-23, 1983, Beijing, pp211-252

[5] D. Yu, Natural Boundary Integral Method and Its Applications, Kluwer Academic Publishers, Massachusetts, 2002

[6] J. B. Keller, and D. Givoli, "Exact Non-reflecting Boundary Conditions," Journal of Computational Physics, vol. 82, no. 1, pp172-192, 1989

[7] M. J. Grote, and J. B. Keller, "On Non-reflecting Boundary Conditions," Journal of Computational Physics, vol. 122, no. 2, pp231-243, 1995

[8] D. Yu, "Approximation of Boundary Conditions at Infinity for a Harmonic Equation," Journal of Computational Mathematics, vol. 3, no. 3, pp219-227, 1985
[9] H. Han, and W. Bao, "Error Estimates for the Finite Element Approximation of Problems in Unbounded Domains," SIAM Journal on Numerical Analysis, vol. 37, no. 4, pp1101-1119, 2000
[10] G. Ben-Poart, and D. Givoli, "Solution of Unbounded Domain Problems using Elliptic Artificial Boundaries," Communications in Numerical Methods in Engineering, vol. 11, no. 9, pp735-741, 1995
[11] D. Yu, and Z. Jia, "Natural Integral Operator on Elliptic Boundaries and a Coupling Method for an Anisotropic Problem," Mathematica Numerica Sinica, vol. 24, no. 3, pp375-384, 2002
[12] Q. Zheng, J. Wang, and J. Li, "The Coupling Method with the Natural Boundary Reduction on an Ellipse for Exterior Anisotropic Problems," Computer Modeling in Engineering and Sciences, vol. 72, no. 2, pp103-113, 2011
[13] H. Han, C. He, and X. Wu, "Analysis of Artificial Boundary Conditions for Exterior Boundary Value Problems in Three Dimensions," Numerische Mathematik, vol. 85, no. 3, pp367-386, 2000
[14] H. Huang, D. Liu and D. Yu, "Solution of Exterior Problem using Ellipsoidal Artificial Boundary," Journal of Computational and Applied Mathematics, vol. 231, no. 1, pp434-446, 2009
[15] D. Yu, "Coupling Canonical Boundary Element Method with FEM to Solve Harmonic Problem over Cracked Domain," Journal of Computational Mathematics, vol. 1, no. 3, pp195-202, 1983
[16] M. Yang, and Q. Du, "A Schwarz Alternating Algorithm for Elliptic Boundary Value Problems in an Infinite Domain with a Concave Angle," Applied Mathematics and Computation, vol. 159, no. 1, pp199-220, 2004
[17] B. Liu, and Q. Du, "The Coupling of NBEM and FEM for Quasilinear Problems in a Bounded or Unbounded Domain with a Cocave Angle," Journal of Computational Mathematics, vol. 31, no. 3, pp308-325, 2013
[18] D. Givoli, L. Rivkin, and J. B. Keller, " A Finite Element Method for Domains with Corners," International Journal for Numerical Methods in Engineering, vol. 35, no. 6, pp1329-1345, 1992
[19] X. Wu, and H. Han, "A Finite Element Method for Laplace and Helmholtz-type Boundary Value Problems with Singularities," SIAM Journal on Numerical Analysis, vol. 34, no. 3, pp1037-1050, 1997
[20] Q. Du, and D. Yu, "Natural Boundary Reduction for Some Elliptic Boundary Value Problems with Concave Angle Domains," Mathematica Numerica Sinica, vol. 25, no. 1, pp85-98, 2003
[21] D. Deng, and T. Pan, "A Fourth-order Singly Diagonally Implicit Runge-Kutta Method for Solving One-dimensional Burgers' Equation," IAENG International Journal of Applied Mathematics, vol. 45, no. 4, pp327-333, 2015
[22] Y. Chen, and Q. Du, "Solution of Exterior Problems using Elliptical Arc Artificial Boundary," Engineering Letters, vol. 24, no. 2, pp202-206, 2016